RSC Advances

ROYAL SOCIETY OF CHEMISTRY

www.rsc.org/advances

Two novel oxovanadium−organophosphonate hybrids with a 3D supramolecular structure: synthesis, crystal structures, surface photovoltage and luminescent properties

Ming–Xue Ma, Zhen–Gang Sun,* Yan–Yu Zhu, Guang–Ning Zhang, Tong Sun, Wen–Zhu Li and Hui Luo

School of Chemistry and Chemical Engineering, Liaoning Normal University, Dalian 116029, P. R. China

Two novel organic–inorganic hybrid materials of oxovanadium−organophosphonate with a 3D supramolecular structure, [{M(1,10−phen)}(VO)(OH)(hedp)]·H_2O (M = Cu (**1**), Zn (**2**); $hedpH_4$ = 1−hydroxyethylidenediphosphonate, 1,10−phen = 1,10−phenanthroline), have been synthesized under hydrothermal conditions. Compounds **1** and **2** are isomorphous and adopt a three−dimensional supramolecular network structure. The interconnection of {$(VO_4)(OH)$}, {MN_2O_3} and {CPO_3} polyhedra leads to a 2D layer through corner−sharing, and such layers are further assembled into a 3D supramolecular structure by π–π stacking interactions. Surface photovoltage and luminescent properties of the two compounds have also been studied.

Introduction

Beyond molecule chemistry, the supramolecular chemistry based on self−assembly of molecular building blocks has received considerable interests mainly due to their potential applications in ion−exchange, catalytic, optical and sensing properties.[1] In the supramolecular materitals, the molecular building blocks are self−assembed *via* intermolecular hydrogen−bonding and/or aromatic π–π stacking interactions and these weaker intermolecular forces play an important role to increase the dimensionality of the polymerization.[2] Much effort has been devoted to the exploration of supramolecular materials with different architectures, particularly the 3D supramolecular structures.[3] As an important part of supramolecular chemistry, polyoxometalates have also attracted much attention on account of their structural diversities and great potential applications.[4] In particular, the chemistry of coordination compounds of polyoxometalates with organic ligands provides knowledge about the interaction of small organic molecules with polyoxometalate surfaces.[5] Actually, the oxovanadium−organophosphonates represent an important subclass of the family of polyoxometalates.[6] Therefore, the rational design and synthesis of oxovanadium−organophosphonates with the intriguing variety of architectures and practical properties have become a particularly important subject.

* To whom correspondence should be addressed: E–mail: szg188@163.com

During the past few years, organodiphosphonate have been proven to be very useful ligands for the preparation of the functionalized polyoxometalates, in which the organic part plays a controllable spacer role and the two inorganic $–PO_3$ groups chelate with metal ions to form 1D, 2D, and 3D structures.[7] With the aim of exploring novel oxovanadium−organophosphonates with interesting structures and properties, we focus our attention on a flexible and multifunctional bisphosphonic acid, 1−hydroxyethylidenediphosphonic acid ($hedpH_4$), which has been widely used as a strong chelating agent in the preparation of functional metal diphosphonates.[8] In this work, by employing 1−hydroxyethylidenediphosphonic acid ($hedpH_4$) as the phosphonate ligand and 1,10−phen as the second metal linker, we have successfully obtained two novel organic–inorganic hybrid materials of oxovanadium−organophosphonate with a 3D supramolecular structure, namely, [{M(1,10−phen)}(VO)(OH)(hedp)]·H_2O (M = Cu (**1**), Zn (**2**)), and surface photovoltage and luminescent properties of the two compounds have also been studied. To date, research on the properties of oxovanadium−organophosphonates is mainly focused on the magnetism; however, there are seldom reports about the photoelectric and luminescent properties of these materials.[9] To the best of our knowledge, this is the first example of the studies on the surface photovoltage and luminescent properties of oxovanadium−organophosphonates. Surface photovoltage spectroscopy (SPS) is an effective tool to investigate the change of the solid surface, which can be used to survey the photophysics of the excited states and the surface charge behavior of the sample.[10] The sensitivity of the method is about 10^8 q/cm^2, which exceeds that of conventional spectroscopies such as XPS and Auger spectroscopy by many orders of magnitude.[11] Recently, only a few investigations on the surface photovoltage properties of oxomolybdenum−organophosphonates have been reported by our group.[12] Herein we report the syntheses, crystal structures, surface photovoltage and luminescent properties of two title compounds.

Experimental

Materials and measurements

1–Hydroxyethylidenediphosphonic acid ($hedpH_4$) solution was obtained from Taihe Chemical Factory (60.0 wt%) and used as received. All other chemicals were obtained from commercial sources and used without further purification. C, H and N were determined by using a PE–2400 elemental analyzer. Cu, Zn, P and V were determined by using an inductively coupled plasma (ICP) atomic absorption spectrometer. IR spectra were recorded on a Bruker AXS TENSOR–27 FT–IR spectrometer with KBr pellets in the range 4000–400 cm^{-1}. Thermogravimetric (TG) analyses were performed on a

Perkin–Elmer Pyris Diamond TG–DTA thermal analyses system in static air with a heating rate of 10 K min^{-1} from 50 °C to 900 °C. The X–ray powder diffraction data was collected on a Bruker AXS D8 Advance diffractometer using Cu–Kα radiation (λ = 1.5418 Å) in the 2θ range of 5–60° with a step size of 0.02° and a scanning rate of 3°/min. Surface photovoltage spectroscopy (SPS) and Field–induced surface photovoltage spectroscopy (FISPS) measurements were conducted with the sample in a sandwich cell (ITO/sample/ITO) with the light source−monochromator−lock−in detection technique in the range of 300–600 nm. The luminescence spectra were reported on a HITACHI F–7000 spectrofluorimeter (solid).

Synthesis of [{Cu(1,10−phen)}(VO)(OH)(hedp)]·H_2O (1). A mixture of $NaVO_3·2H_2O$ (0.07 g, 0.45 mmol), $CuCl_2·2H_2O$ (0.12 g, 0.70 mmol), 1,10−phenanthroline (0.08 g, 0.43 mmol) and $hedpH_4$ solution (0.12 mL, 0.30 mmol) was dissolved in 8 mL distilled water. The resulting solution was stirred for about 1 hour at room temperature, sealed in a 20 mL Teflon–lined stainless steel autoclave, and heated at 160 °C for 72 h under autogenous pressure. After the mixture was cooled slowly to room temperature, the green block crystals were obtained. Yield 78.6 % (based on V). Anal. Calc. for $C_{14}H_{15}CuN_2O_{10}P_2V$: C, 30.70; H, 2.76; N, 5.11; P, 11.31; Cu, 11.60; V, 9.30. Found: C, 30.75; H, 2.72; N, 5.14; P, 11.35; Cu, 11.55; V, 9.27 %. IR (KBr, cm^{-1}): 3478(m), 3176(m), 3070(w), 2961(w), 1668(w), 1512(w), 1426(w), 1115(s), 1104(m), 989(m), 853(w), 727(w), 571(m), 454(m).

Synthesis of [{Zn(1,10−phen)}(VO)(OH)(hedp)]·H_2O (2). A mixture of $NaVO_3·2H_2O$ (0.05 g, 0.33 mmol), $ZnSO_4·7H_2O$ (0.15 g, 0.52 mmol), 1,10−phenanthroline (0.10 g, 0.5 mmol) and $hedpH_4$ solution (0.30 mL, 0.72 mmol) was dissolved in 8 mL distilled water. The resulting solution was stirred for about 1 hour at room temperature, sealed in a 20 mL Teflon–lined stainless steel autoclave, and heated at 160 °C for 72 h under autogenous pressure. After the mixture was cooled slowly to room temperature, the green block crystals were obtained. Yield 64.3 % (based on V). Anal. Calc. for $C_{14}H_{15}ZnN_2O_{10}P_2V$: C, 30.60; H, 2.75; N, 5.09; P, 11.27; Zn, 11.90; V, 9.26. Found: C, 30.64; H, 2.72; N, 5.05; P, 11.33; Zn, 11.86; V, 9.27 %. IR (KBr, cm^{-1}): 3428(m), 3186(w), 3079(w), 1621(m), 1512(w), 1426(w), 1106(s), 1056(m), 1007(m), 980(m), 842(w), 715(w), 580(m), 492(m).

Crystallographic studies

Data collections for compounds **1** and **2** were performed on the Bruker AXS Smart APEX II CCD X−diffractometer equipped with graphite monochromated Mo−*Kα* radiation (λ = 0.71073 Å) at 293 ±

2K. An empirical absorption correction was applied using the SADABS program. All structures were solved by direct methods and refined by full−matrix least squares fitting on F^2 by SHELXS−97.[13] All non−hydrogen atoms were refined anisotropically. Hydrogen atoms except those for water molecules were generated geometrically with fixed isotropic thermal parameters and included in the structure factor calculations. Hydrogen atoms for water molecules were not included in the refinement. Details of crystallographic data and structural refinements of compounds **1** and **2** are summarized in Table 1. Selected bond lengths and angles of compounds **1** and **2** are listed in Table S1.

Results and discussion

Syntheses

Two novel oxovanadium−organophosphonate materials have been successfully synthesized by hydrothermal methods. Product composition depends on a number of critical conditions, including the initial reactants, molar ratio, pH value, reaction time and temperature in the process of hydrothermal synthesis. With the aim to obtain good samples for X−ray diffraction studies, the optimal conditions of synthesizing were explored. It was found that the molar ratio of starting materials plays an important role in the growth of these compounds. The pure phases of compound **1** were obtained in regions with the molar ratio $NaVO_3{\cdot}2H_2O/CuCl_2{\cdot}2H_2O$/1,10−phen/$hedpH_4$ = 3:5:3:2. Despite our efforts to grow single crystals of compound **1** with other molar ratios, no good samples for X−ray diffraction study were obtained. We try to prepare compound **2** following the same molar ratio of compound **1**, only a few green powder was observed. Finally, the best crystals of compound **2** were isolated in regions with the molar ratio $NaVO_3{\cdot}2H_2O/ZnSO_4{\cdot}7H_2O$/1,10−phen/$hedpH_4$ = 3:5:5:7. However, the formation of powders or mixture phases (tiny crystals and powders) for compound **2** comes into being at other molar ratio. In addition, the reaction temperature also has a strong effect on the formation of the compounds. Larger crystals of compounds **1** and **2** were obtained at the used reaction temperature of 160 °C. Compound **2** can also be obtained at 120 °C and 140 °C, but the quality is not good enough for single−crystal structure determination. We also tried to prepared compound **1** under the same synthesis conditions at different temperatures, but impure crystals or powders were obtained. It is needless to adjust the pH values of the reaction mixtures for the syntheses of compounds **1** and **2**. The detailed exploration of optimum experimental conditions of compounds **1** and **2** are listed in Table S2. The powder XRD patterns and the simulated XRD patterns of the two compounds are shown in the ESI (Fig. S3, ESI). The diffraction peaks on the patterns correspond well in position, confirming that the two compounds are all pure phase. The differences in reflection intensity are probably due to preferred orientation in the powder samples.

Table 1

Description of the crystal structures

Single−crystal X−ray diffraction analysis reveals that compounds **1** and **2** are isostructural and crystallize in the monoclinic space group *C*2/c (Table 1). Hence only the structure of compound **1** will be discussed in detail as a representation. As shown in Fig. 1, The V(1) is five−coordinated by three phosphonate oxygen atoms (O2, O5, O3A) from two separate $hedp^{4-}$ anions [V(1)−O(2) = 2.015(4), V(1)−O(5) = 1.965(3), V(1)−O(3A) = 1.970(3) Å], one terminal oxygen atom [V(1)−O(9) = 1.597(4) Å], and one hydroxyl group [V(1)−O(8) = 2.059(4) Å] form a {$(VO_4)(OH)$} cluster. The Cu(1) ion is also five−coordinated by two nitrogen atoms (N1, N2) from the 1,10−phenanthroline ligand [Cu−N = 2.028(5) Å], three oxygen atoms (O1, O4, O6B) from two separate $hedp^{4-}$ anions [Cu(1)−O(1) = 1.977(3), Cu(1)−O(4) = 1.936(4), Cu(1)−O(6B) = 2.152(3) Å] (Table S1). These values are in agreement with those reported for other oxovanadium−organophosphonate.[14] In compound **1**, the phosphonate oxygen atoms of $hedp^{4-}$ are all coordinated. Each $hedp^{4-}$ ligand links two vanadium center and two copper subunits (Fig. S1, ESI).

Fig. 1

Fig. 2

The overall structure of compound **1** can be described as a 3D supramolecular structure. As shown in Fig. 2, two {$(VO_4)(OH)$} square pyramidal and two {CuN_2O_3} square pyramidal are linked by {CPO_3} tetrahedra through phosphonate oxygen atoms to form a $[Cu(1,10-phen)(VO)(OH)(hedp)]_2$ unit *via* corner–sharing. Such units are cross−linked by $hedp^{4-}$ anions through phosphonate oxygen atoms into a 2D layer in the *bc*–plane. The result of connections in this manner is the formation of an 24−atom window, which consists of two V, four Cu, six P and twelve C atoms with the sequences $\{V–O–P–O–Cu–O–P–O–Cu–O–P–O–\}_2$. The dimensions of the windows are estimated to be 6.9 Å (V1–V1) × 12.1 Å (Cu1–Cu1) based on structure data. Then the adjacent layers are further assembled into a 3D supramolecular structure through π−π stacking interactions (Fig. 3). The π–π stacking

interactions can play an important role in controlling the packing or assembly of compounds. The usual π–π interaction is an offset or slipped stacking of the aromatic nitrogen heterocycles or benzene rings, and the effective distance for such interactions is about 3.3–3.8 Å.[15] In compound **1**, the 1,10−phen rings between the neighboring asymmetric unit are parallel to each other, and the face−to−face distance (3.65 Å) between adjacent 1,10−phen rings is in the normal range for such interactions, hence there are π−π stacking interactions.

Fig. 3

IR spectroscopy

The IR spectra for compounds **1** and **2** are recorded in the region 4000−400 cm^{-1} (Fig. S2, ESI). The IR spectra of the two compounds have many similar features corresponding to the common groups, thus only the spectrum of compound **1** will be discussed. The absorption band at 3478 cm^{-1} can be as signed to the O–H stretching vibrations of water molecules and hydroxyl groups.[16a] Sharp bands located at about 3000 cm^{-1} are due to the C–H stretching vibrations. The bands at 1668, 1512, 1426 cm^{-1} can be assigned to the stretching bands of the 1,10−phenanthroline ligands.[15b, 16b] Absorption band at 989 cm^{-1} is attribute to ν(V=O).[16c] The set of bands between 1200 and 900 cm^{-1} are due to stretching vibrations of the tetrahedral CPO_3 groups, as expected.[16d] Additional medium and weak bands at low energies are found, which are likely assigned to bending vibrations of the tetrahedral CPO_3 groups.

Fig. 4

Thermal analyses

In order to examine the thermal stabilities of compounds **1** and **2**, thermogravimetric analyses were performed in the temperature range of 50–900 °C under static air atmosphere (Fig. S4, ESI). The TG−DTG curves of compounds **1** and **2** are nearly similar and we use compound **1** as an example to illuminate the weight losses in detail. The TG curve of compound **1** indicates two main steps. It shows no weight loss from room temperature to 232 °C. The first step started at 232 °C and was completed at 272 °C, which can be attributed to the release of one lattice water molecule and partial decomposition

of organic groups. The second step, from 272 to 583 °C, corresponding to further decomposition of the compound. Although the TG−DTG curve reveals a multistep decomposition process above the temperature of 272 °C, it can be regarded as a continuous and complicated weight loss. The total weight loss at 583 °C is 42.8%. For compound **2**, the total weight loss at 743 °C is 45.3%. The product of the thermal decomposition is amorphous and was not further characterized.[17] To further understand the thermal stability of compounds **1** and **2**, X−ray powder diffraction studies were performed from 140 to 230 °C. As shown in Fig. 4, the powder XRD patterns demonstrate the retention of the framework structure of compound **1** below 210 °C. For compound **2** the pattern changes when the temperature reaches 210 °C, which indicates that the structure of compound **2** was thermally stable below 200 °C.

Surface photovoltage properties

Surface photovoltage spectroscopy (SPS) is an effective technique that can be used to investigate the photophysics of the excited states and the surface charge behavior of the sample. It not only relates to the electron transitions under light inducement, but also reflects the separation and transfer of photo−generated charges as well as the optical absorption characteristics of semiconductor samples.[18] The principle and the scheme are described elsewhere.[19] The detected SPS signal is equivalent to the change in the surface potential barrier on illumination (δVs), which is given by the equation: $\delta Vs = V's - V^{o}s$, where $V's$ and $V^{o}s$ are the surface potential barriers before and after illumination, respectively. As far as band to band transitions are concerned, a positive response of surface photovoltage (SPV) ($\delta Vs > 0$) means that the sample is characterized as a *p*−type semiconductor, whereas a negative response corresponds to an *n*−type semiconductor.[20]

Fig. 5

Fig. 6

The magnitude of the surface potential barrier depends on the numbers of surface net charge. Fig. 5 shows the SPS spectra of compounds **1** and **2**. They all appear as positive SPV response bands between 300 and 600 nm. It can be seen that the signal detected by SPS at 300–400 nm is a wide peak. The signal is actually the result of overlap of several SPV response bands. To make the assignment of each SPV response band clear, we separated them by the Origin 7.0 program. The compound **1** presents two positive SPV responses at 322 and 341 nm (Fig. 5a). The response at λ_{max} = 322 nm is attributed to the $\pi \rightarrow \pi^*$ transition of $\{Cu(phen)\}^{2+}$, while the response at λ_{max} = 341 nm can be assigned to the LMCT

(O→V). The SPS of compound **2** is similar to that of compound **1**. After Origin 7.0 treatment, two response bands at 322 and 353 nm were observed (Fig. 5b). The former response band at 322 nm may be assigned to the π→π* transition of $\{Zn(phen)\}^{2+}$ and the latter band is attributed to the LMCT (O→V). The surface photovoltage spectra of compounds **1** and **2** indicate that not only semiconductor possess photovoltage characteristics, some materials with the semiconductor characteristic (such as coordination polymers) also can exhibit the photovoltage property. Therefore, oxovanadium−organophosphonates can be regarded as a kind of extended novel semiconductors.

Field−induced surface photovoltage spectroscopy (FISPS) can be measured by applying an external electric field to the sample with a transparent electrode. For a *p*−type semiconductor, when a positive electric field is applied on the semiconductor surface, the SPV response increases since the external field is consistent with the built−in field. On the contrary, when a negative electric field is applied, the SPV response is weakened. In contrast to *p*−type semiconductors, the SPV response intensity of *n*−type semiconductor increases as a negative field is applied and reduces as a positive electric field is applied. Fig. 6 shows the FISPS of compounds **1** and **2** in the range of 300–600 nm when the external electric fields are −0.2, 0, and +0.2 V, respectively. The SPV response intensities of the two compounds increase when the positive fields increase, while they reduce when the external negative fields increase. This is attributed to the positive electric field being beneficial to the separation of photoexcited electron–hole pairs, which in turn results in an increase of response intensity; however, the negative electric field has just the opposite effect. The FISPS confirms the *p*−type characteristics of compounds **1** and **2**.

Luminescent properties

The luminescent behaviors of compounds **1** and **2** were investigated in the solid state at room temperature. The free $hedpH_4$ ligand exhibits an emission band at 393 nm (λ_{ex} = 318 nm) (Fig. S5, ESI), while the free 1,10−phen ligand displays luminescence with two emission maximum at 397 and 449 nm (λ_{ex} = 260 nm). As shown in Fig. 7, compound **1** exhibits a shoulder weaker emission peak at 374 nm and a broad emission band between 350 and 450 nm with a maximum peak at 415 nm (λ_{ex} = 260 nm). Under the same experimental conditions, compound **2** displays luminescence with two emission maximum at 375 and 409 nm. It is clear that compounds **1** and **2** show a red−shifted emission band with different extents weakened intensities compared with the free 1,10−phen ligand, which probably originated from ligand−to−metal charge transfer (LMCT).[21] The free $NaVO_3{\cdot}2H_2O$ shows a strong fluorescent emission band at 468 nm (λ_{ex} = 260 nm), and the emission peaks at 468 nm for compounds **1** and **2** may be attributable to internal transitions of the oxovanadium anions. The luminescent

intensity of compound **2** is stronger than that of compound **1**, which is probably due to the coordination to different metal ions, because the luminescence behavior is closely associated with the metal ions.[22] Luminescent properties of compounds **1** and **2** indicate that they are good candidates for blue−light luminescent materials.

Fig. 7

Conclusions

In this study, two novel organic−inorganic hybrid materials of the oxovanadium−organophosphonate with a 3D supramolecular structure, [{M(1,10−phen)}(VO)(OH)(hedp)]·H_2O (M = Cu (**1**), Zn (**2**)) have been synthesized by the hydrothermal technique. Compounds **1** and **2** are isomorphous and adopt a three−dimensional supramolecular network structure. The interconnection of {(VO_4)(OH)}, {MN_2O_3} and {CPO_3} polyhedra leads to a 2D layer through corner−sharing, and such layers are further assembled into a 3D supramolecular structure by π−π stacking interactions. The SPS and FISPS of compounds **1** and **2** indicate that they exhibit surface photovoltage properties and show *p*−type semiconductor characteristics. Therefore, oxovanadium−organophosphonates hybrids can be regarded as a kind of novel photoelectric material. The luminescent analysis indicates that compounds **1** and **2** may be good candidates for blue−light luminescent materials.

Acknowledgement

This work is supported by the National Natural Science Foundation of China (Grant No. 21371085).

Electronic supplementary information (ESI) available: X−ray crystallographic files in CIF format for compounds **1** and **2**. Exploration of optimum experimental conditions of compounds **1** and **2**. Coordination mode of $hedpH_4$ in compound **1**. IR spectra of compounds **1** and **2**. XRD patterns of the experiments compared to those simulated from X−ray single−crystal data for compounds **1** and **2**. TG−DTG curves of compounds **1** and **2**. Solid–state luminescent property of the free $HedpH_4$ ligand. CCDC 1011164 (**1**) and 1011165 (**2**) contain the supplementary crystallographic data for this paper. These data can be obtained free of charge www.ccdc.cam.ac.uk/conts/retrieving.html (or from the Cambridge Crystallographic Data Center, 12, Union Road, Cambridge CB21EZ, UK; fax: (+44) 1223–336–033; e–mail: deposit@ccdc.cam.ac.uk).

Notes and references

1 (a) J. M. Lehn, *Chem. Soc. Rev*., 2007, **36**, 151. (b) D. Kong, J. L. McBee and A. Clearfield, *Cryst. Growth Des*., 2005, **5**, 643. (c) F. P. Zhai, Q. S. Zheng, Z. X. Chen, Y. Ling, X. F. Liu, L. H. Weng and Y. M. Zhou, *CrystEngComm*., 2013, **15**, 2040. (d) C. V. K. Sharma and A. Clearfield, *J. Am. Chem. Soc*., 2002, **122**, 4394.

2 (a) Y. Cui, H. L. Ngo, P. S. White and W. B. Lin, *Inorg. Chem*., 2003, **42** 652. (b) J. C. Noveron, M. S. Lah, R. E. D. Sesto, A. M. Miller, J. S. Miller and P. J. Stang, *J. Am. Chem. Soc*., 2002, **124**, 6613. (c) S. L. Zheng, M. L. Tong, R. W. Fu, X. M. Chen and S. W. Ng, *Inorg. Chem*., 2001, **40**, 3562.

3 (a) H. Zhu, J. Huang, S. S. Bao, M. Ren and L. M. Zheng, *Dalton Trans*., 2013, **42**, 14075. (b) C. Li, C. Q. Jiao, Z. G. Sun, K. Chen, C. L. Wang, Y. Y. Zhu, J. Zhu, Y. Zhao, M. J. Zheng, S. H. Sun, W. Chu and H. Tian, *CrystEngComm*., 2012, **14**, 5479. (c) L. H. Schilling and N. Stock, *Dalton Trans*., 2014, **43**, 414.

4 (a) W. P. Deng, Q. H. Zhang and Y. Wang, *Dalton Trans*., 2012, **41**, 9817. (b) C. Pichon, A. Dolbecq, P. Mialane, J. Marrot, E. Rivière, M. Goral, M. Zynek, T. McCormac, S. A. Borshch, E. Zueva and F. Sécheresse, *Chem. Eur. J*., 2008, **14**, 3189. (c) W. Ouellette, M. H. Yu, C. J. O'Connor and J. Zubieta, *Inorg. Chem*., 2006, **45**, 3224. (d) D. E. Katsoulis, *Chem. Rev*., 1998, **98**, 359. (e) C. Streb, C. Ritchie, D. L. Long, P. Kögerler and L. Cronin, *Angew. Chem. Int. Ed*., 2007, **46**, 7579.

5 (a) H. X. Yang, S. P. Guo, J. Tao, J. X. Lin and R. Cao, *Cryst. Growth Des*., 2009, **9**, 4735. (b) J. Rocha, F. A. A. Paz, F. N. Shi, R. A. S. Ferreira, T. Trindade and L. D. Carlos, *Eur. J. Inorg. Chem*., 2009, **33**, 4931. (c) C. G. Werncke, C. Limberg, C. Knispel, R. Metzinger and B. Braun, *Chem. Eur. J*., 2011, **17**, 2931. (d) A. M. Douvas, K. Yannakopoulou and P. Argitis, *Chem. Mater*., 2010, **22**, 2730.

6 (a) W. Ouellter, M. H. Yu, C. J. O'Connor and J. Zubieta, *Inorg. Chem*., 2006, **45**, 7628. (b) J. Thomas, M. Agarwal, A. Ramanan, N. Chernova and M. S. Whittingham, *CrystEngComm*., 2009, **11**, 625. (c) X. M. Zhang, J. J. Hou, W. X. Zhang and X. M. Chen, *Inorg. Chem*., 2006, **45**, 8120.

7 (a) N. G. Armatas, D. G. Allis, A. Prosvirin, G. Carnutu, C. J. O'Connor, K. Dunbar and J. Zubieta, *Inorg. Chem*., 2008, **47**, 832. (b) R. C. Finn, E. Burkholder and J. Zubieta, *Chem. Commun*., 2001, 1852. (c) W. Owellette, G. B. Wang, H. X. Liu, G. T. Yee, C. J. O'Connor and J. Zubieta, *Inorg. Chem*., 2009, **48**, 953.

8 (a) H. Tian, Y. Y. Zhu, Z. G. Sun, F. Tong, J. Zhu, W. Chu, S. H. Sun and M. J. Zheng, *New. J. Chem*., 2013, **37**, 212. (b) D. K. Cao, M. J. Liu, J. Huang, S. S. Bao and L. M. Zheng, *Inorg.*

Chem., 2011, **50**, 2278.

9 (a) S. Ushak, E. Spodine, E. L. Fur, D. V. Yazigi, J. Y. Pivan, W. Schnelle, R. C. Gil and R. Kniep, *Inorg. Chem*., 2006, **45**, 5393. (b) P. DeBurgomaster, W. Ouellette, H. Liu, C. J. O'Connor and J. Zubieta, *CrystEngComm*., 2010, **12**, 446.

10 L. Kronik and Y. Shapira, *Surf. Sci. Rep*., 1999, **37**, 1.

11 K. X. Wang and J. S. Chen, *Acc. Chem. Res*., 2011, **44**, 531.

12 S. H. Sun, Z. G. Sun, Y. Y. Zhu, D. P. Dong, C. Q. Jiao, J. Zhu, J. Li, W. Chu, H. Tian, M. J. Zheng, W. Y. Shao and Y. F. Lu, *Cryst. Growth Des*., 2013, **13**, 226.

13 G. M. Sheldrick, *SHELXS−97, Program for X−ray Crystal Structure Solution and Refinement*, University of Göttingen, Germany, 1997.

14 B. K. Tripuramallu and S. K. Das, *Cryst. Growth Des*., 2013, **13**, 2426.

15 (a) C. Janiak, *Dalton Trans*., 2000, 3885. (b) L. L. Dai, Y. Y. Zhu, C. Q. Jiao, Z. G. Sun, S. P. Shi, W. Zhou, W. Z. Li, T. Sun, H. Luo and M. X. Ma, *CrystEngComm*., 2014, **14**, 5050.

16 (a) Z. M. Sun, B. P. Yang, Y. Q. Sun, J. G. Mao and A. Clearfield, *J. Solid State Chem*., 2003, **176**, 62. (b) R. T. Clarke, K. Latham, C. J. Rix and M. Hobday, *Chem. Mater*., 2004, **16**, 2463. (c) W. Owellette, V. Golub, C. J. O'Connor and J. Zubieta, *J. Solid. State. Chem*., 2007, **180**, 2500. (d) A. Cabeza, X. Ouyang, C. V. K. Sharma, M. A. G. Aranda, S. Bruque and A. Clearfield, *Inorg. Chem*., 2002, **41**, 2325.

17 M. Li, J. F. Xiang, S. M. Wu, S. P. Chen, L. J. Yuan, H. Li, H. J. He and J. T. Sun, *J. Mol. Struct*., 2007, **840**, 119.

18 (a) Y. H. Lin, D. J. Wang, Q. D. Zhao, M. Yang and Q. L. Zhang, *J. Phys. Chem. B*, 2004, **108**, 3202. (b) B. F. Xin, L. Q. Jing, Z. Y. Ren, B. Q. Wang and H. G. Fu, *J. Phys. Chem. B*, 2005, **109**, 2805.

19 (a) J. Zhang, D. J. Wang, Y. M. Chen, T. J. Li, H. F. Mao, H. J. Tian, Q. F. Zhou and H. J. Xu, *Thin Solid Films*, 1997, **300**, 208. (b) L. Q. Jing, X. J. Sun, J. Shang, W. M. Cai, Z. L. Xu, Y. G. Du and H. G. Fu, *Sol. Energy Mater. Sol. Cells*, 2003, **97**, 133.

20 L. Li, S. Y. Niu, D. Li, J. Jin, Y. X. Chi and Y. H. Xing, *Inorg. Chem. Commun*., 2011, **14**, 993.

21 (a) J. C. Dai, X. T. Wu, Z. Y. Fu, C. P. Cui, S. M. Hu, W. X. Du, L. M. Wu, H. H. Zhang and R. Q. Sun, *Inorg. Chem*., 2002, **41**, 1391. (b) W. Chu, Z. G. Sun, C. Q. Jiao, Y. Y. Zhu, S. H. Sun, H. Tian and M. J. Zheng, *Dalton Trans*., 2013, **42**, 8009.

22 Y. Gong, W. Tang, W. B. Hou, Z. Y. Zha and C. W. Hu, *Inorg. Chem*., 2006, **45**, 4987.

Table 1 Crystal data and structure refinements for compounds **1** and **2**.

Compounds	**1**	**2**
Empirical Formula	$C_{14}H_{15}CuN_2O_{10}P_2V$	$C_{14}H_{15}ZnN_2O_{10}P_2V$
F*w*	547.70	549.53
Crystal system	Monoclinic	Monoclinic
Space group	*C*2/c	*C*2/c
a (Å)	24.702(4)	24.737(4)
b (Å)	9.1070(12)	9.1709(15)
c (Å)	20.913(3)	20.942(4)
β (°)	124.178(2)	121.807(3)
V (Å^3)	3892.0(9)	4037.5(12)
Z	8	8
D_{calcd} (Mg m^{-3})	1.869	1.808
μ (mm^{-1})	1.795	1.865
F(000)	2200	2208
Crystal size/mm	0.09 x 0.06 x 0.05	0.04 x 0.03 x 0.02
Theta range (°)	1.99 to 24.49	1.94 to 26.50
Reflections collected/unique	9118, 3243 (R_{int} = 0.0710)	11216, 4189 (R_{int} = 0.0518)
GOF on F^2	1.015	1.018
R_1, wR_2 [a] [I>2σ (I)]	0.0483, 0.0889	0.0424, 0.0888
R_1, wR_2 [a] (all data)	0.0901, 0.1053	0.0823, 0.1042

[a] $R_1 = \Sigma\,(|F_0|-|F_C|) / \Sigma\,|F_0|$; [b] $wR_2 = [\Sigma\, w\,(|F_0|-|F_C|)^2 / \Sigma\, w\, F_0^2]^{1/2}$.

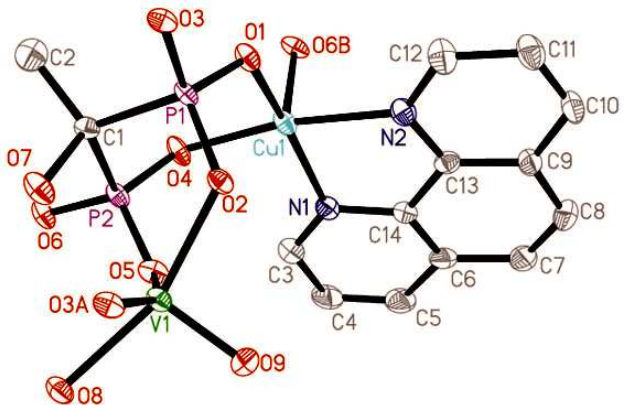

Fig. 1 Structure unit of compound **1** showing the atom labeling. Thermal ellipsoids are shown at the 50% probability level. All H atoms and lattice water molecules are omitted for clarity. Symmetry code for the generated atoms: (A) −x + 1/2, −y +1/2, −z; (B) −x + 1/2, y + 1/2, −z + 1/2.

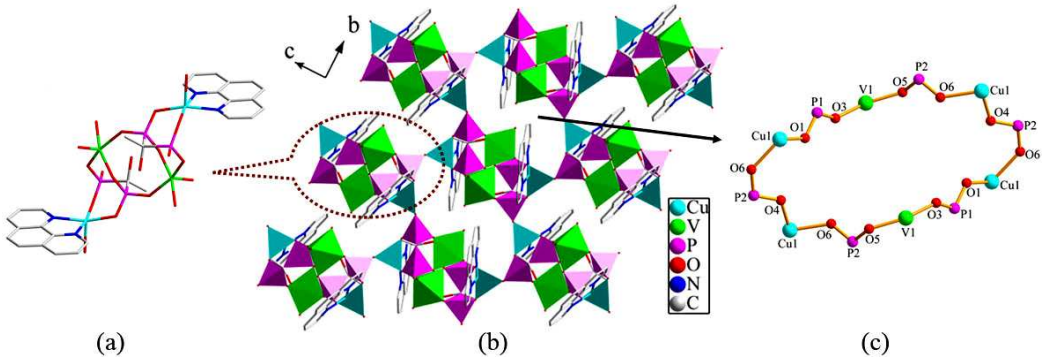

Fig. 2 (a) View of the [Cu(1,10−phen)(VO)(OH)(hedp)]$_2$ unit of compound **1**; (b) View of the layer structure for compound **1** in the *bc*−plane; (c) A 24−atom rings in compound **1**.

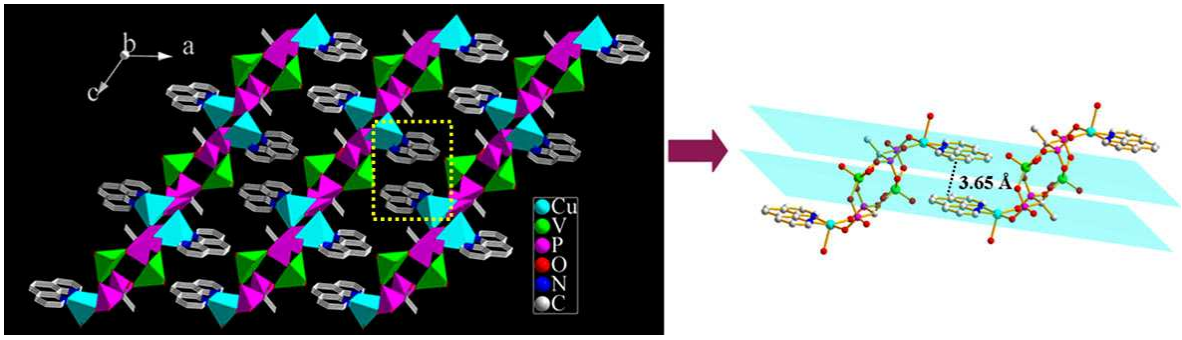

Fig. 3 A view of the three−dimensional supramolecular structure *via* the π−π stacking interactions. The π−π stacking interactions between the adjacent 1,10−phen rings with the face−to−face distance of 3.65 Å.

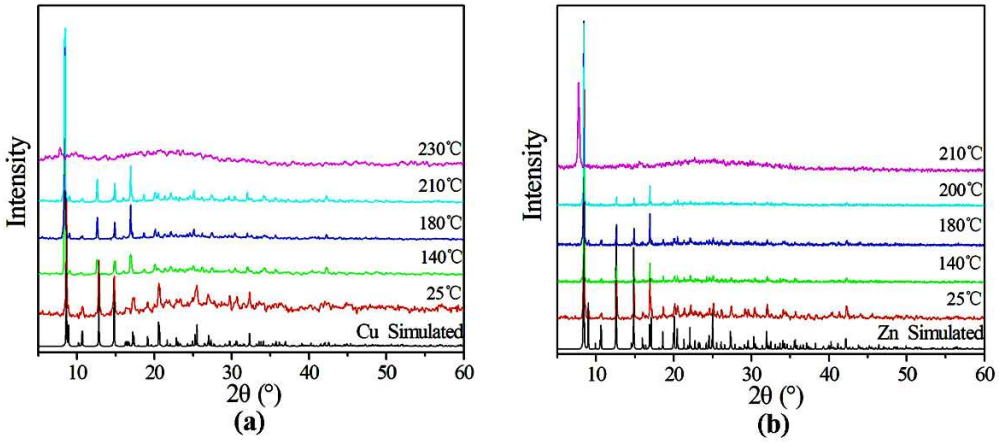

Fig. 4 PXRD patterns for (a) **1** on heating from 25–230 °C and (b) **2** on heating from 25–210 °C.

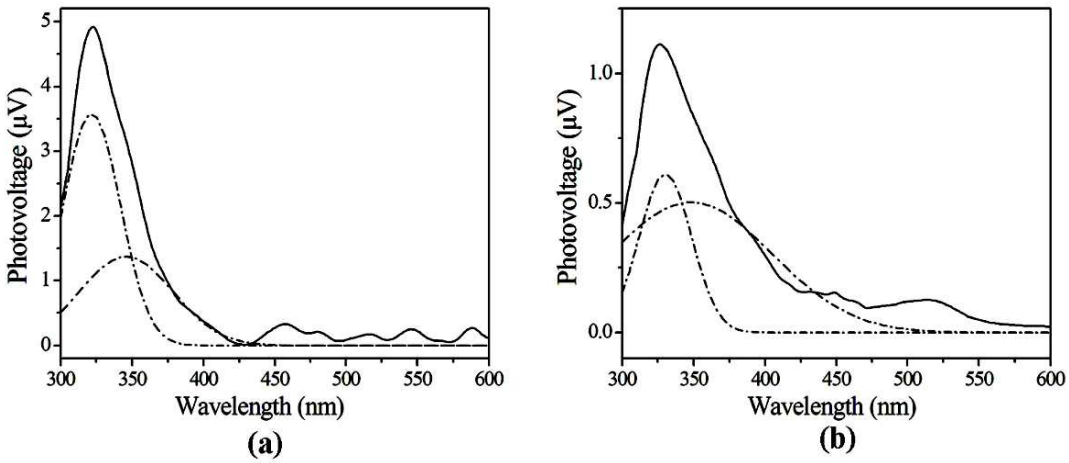

Fig. 5 The SPS of compounds **1** (a), **2** (b). Dotted lines are treated peak.

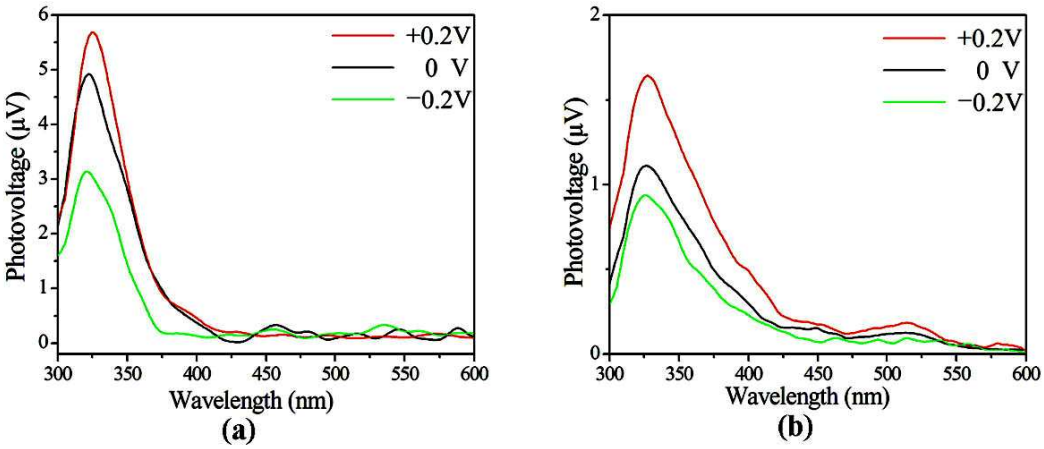

Fig. 6 The FISPS of compounds **1** (a), **2** (b).

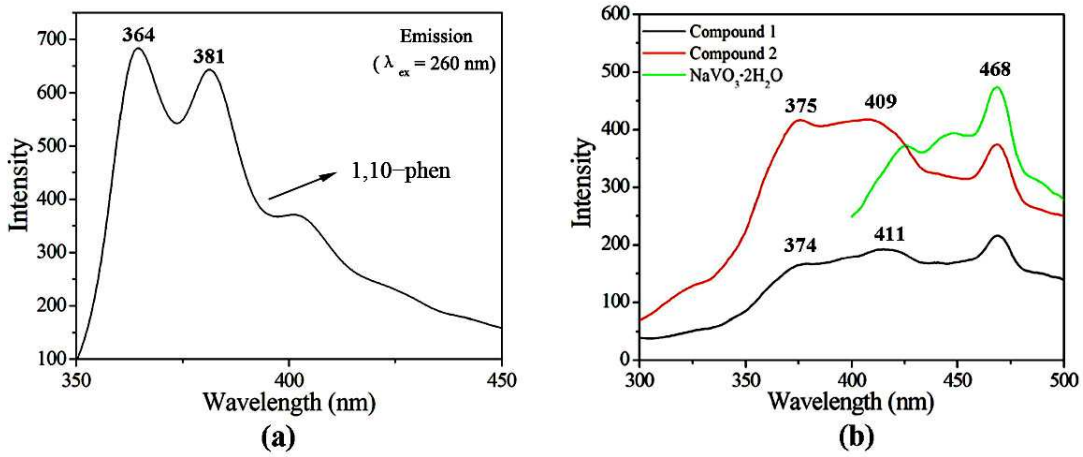

Fig. 7 (a) Solid−state emission spectrum of 1,10−phen at room temperature; (b) Solid−state emission spectra of $NaVO_3 \cdot 2H_2O$ (green line), compound **1** (black line) and compound **2** (red line) at room temperature.

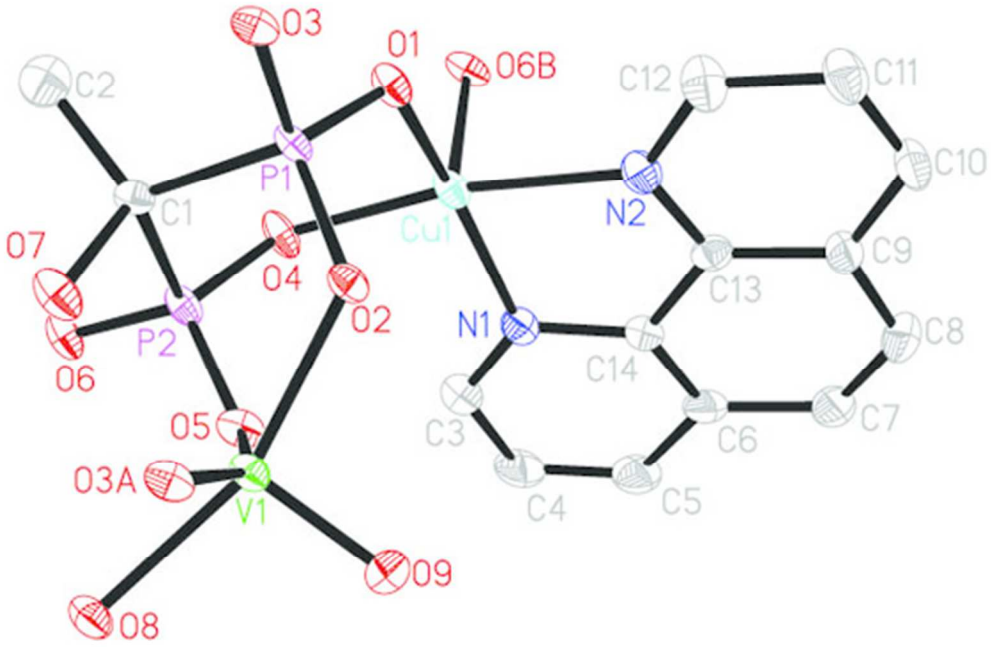

200x131mm (72 x 72 DPI)

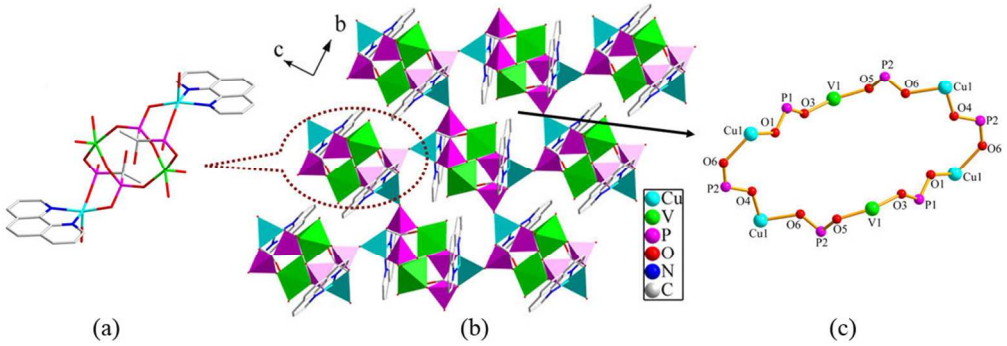

199x69mm (150 x 150 DPI)

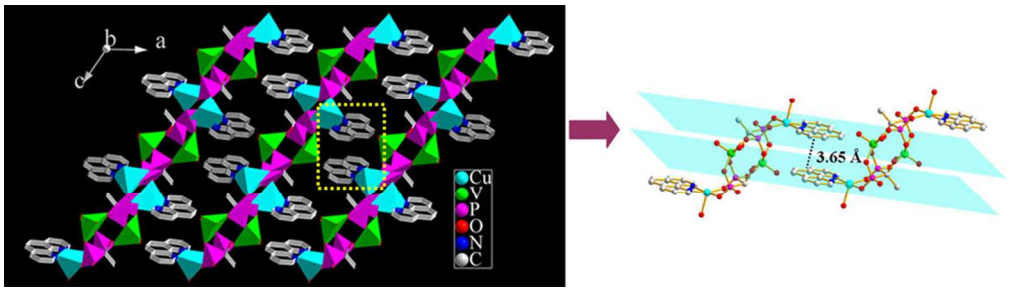

199x56mm (150 x 150 DPI)

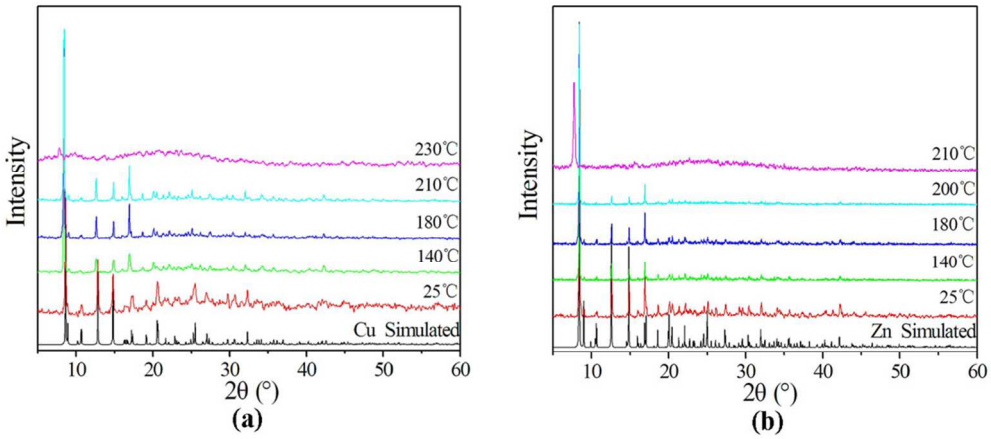

199x89mm (150 x 150 DPI)

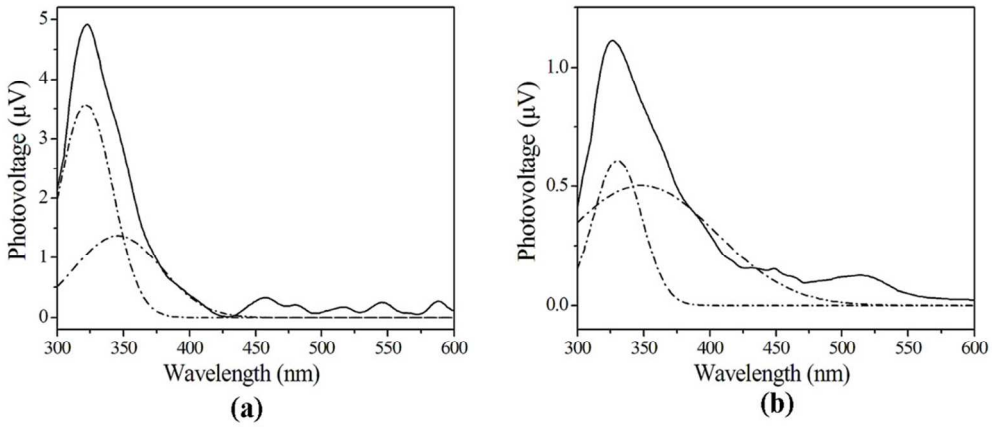

199x87mm (150 x 150 DPI)

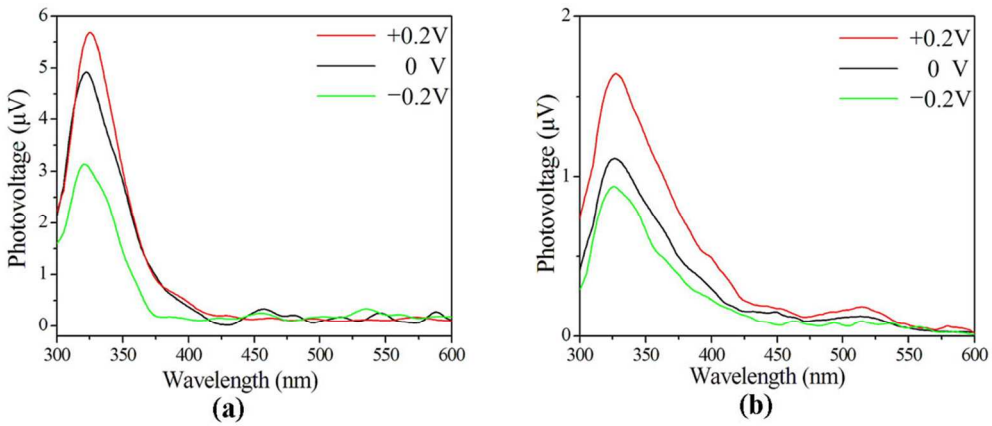

199x85mm (150 x 150 DPI)

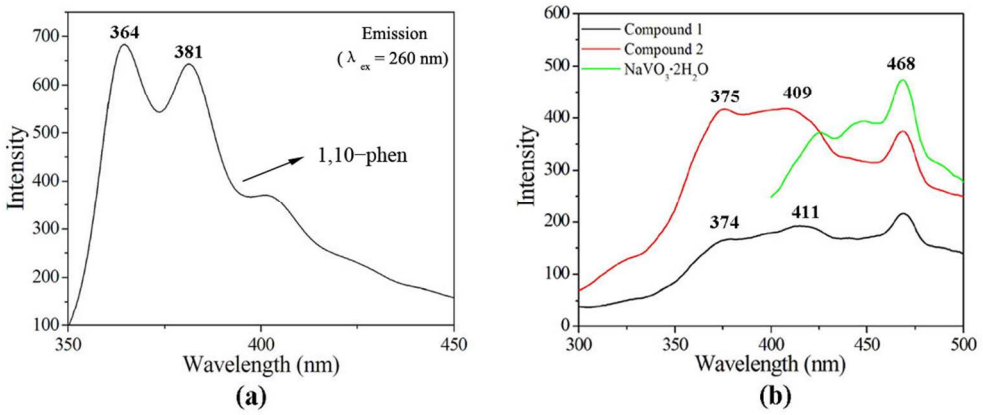

199x85mm (150 x 150 DPI)

Table 1 Crystal data and structure refinements for compounds **1** and **2**.

Compounds	**1**	**2**
Empirical Formula	$C_{14}H_{15}CuN_2O_{10}P_2V$	$C_{14}H_{15}ZnN_2O_{10}P_2V$
F*w*	547.70	549.53
Crystal system	Monoclinic	Monoclinic
Space group	*C*2/c	*C*2/c
a (Å)	24.702(4)	24.737(4)
b (Å)	9.1070(12)	9.1709(15)
c (Å)	20.913(3)	20.942(4)
β (°)	124.178(2)	121.807(3)
V (Å^3)	3892.0(9)	4037.5(12)
Z	8	8
D_{calcd} (Mg m^{-3})	1.869	1.808
μ (mm^{-1})	1.795	1.865
F(000)	2200	2208
Crystal size/mm	0.09 x 0.06 x 0.05	0.04 x 0.03 x 0.02
Theta range (°)	1.99 to 24.49	1.94 to 26.50
Reflections collected/unique	9118, 3243 (R_{int} = 0.0710)	11216, 4189 (R_{int} = 0.0518)
GOF on F^2	1.015	1.018
R_1, wR_2 [a] [I>2σ (I)]	0.0483, 0.0889	0.0424, 0.0888
R_1, wR_2 [a] (all data)	0.0901, 0.1053	0.0823, 0.1042

[a] $R_1 = \Sigma (|F_0|-|F_C|) / \Sigma |F_0|$; [b] $wR_2 = [\Sigma w (|F_0|-|F_C|)^2 / \Sigma w F_0^2]^{1/2}$.

Graphical Abstract

Two novel organic–inorganic hybrid materials of oxovanadium−organophosphonates with a 3D supramolecular structure, [{M(1,10−phen)}(VO)(OH)(hedp)]·H_2O (M = Cu (**1**), Zn (**2**); hedpH_4 = 1−hydroxyethylidenediphosphonate, 1,10−phen = 1,10−phenanthroline), have been synthesized under hydrothermal conditions. Compounds **1** and **2** are isomorphous and adopt a three−dimensional supramolecular network structure. The interconnection of {(VO_4)(OH)}, {MN_2O_3} and {CPO_3} polyhedra leads to a 2D layer through corner−sharing, and such layers are further assembled into a 3D supramolecular structure by π–π stacking interactions. Surface photovoltage and luminescent properties of the two compounds have also been studied.